

# The Workability of Melamine Coated Particle Boards Part II

Bolesław PORANKIEWICZ\* and Chiaki TANAKA\*\*

\*Agricultural University of Poznań, Department of Woodworking Machinery & Machines Constructions  
Bases, Wojska Polskiego 38/42, 60 627 Poznań, Poland

\*\*Department of Natural Resources Process Engineering

## Abstract

The experimental matrix from previous work [5] was expanded by a high temperature corrosion effect (HTC) of particleboard towards a binder in cemented carbide, expressed by quantifier ( $R_{MSMI}$ ). A new multivariable analysis was developed, incorporating a complete model of cutting edge wear ( $h^P$ ) from a cutting path ( $C_P$ ), sharpness ( $\beta_F$ ) and rake ( $\gamma_F$ ) angles, content ( $S_{AC}$ ), weighted average size of particles ( $W_{ASS}$ ) of mineral contamination, a quantifier ( $R_{MSMI}$ ) and a porosity fraction ( $P_S$ ). A model of the functional dependence  $h^P = f(C_P, C_S, \beta_F, \gamma_F, R_{MSMI}, S_{AC}, W_{ASS}, P_S)$  during coated particle board longitudinal milling was developed. The HTC effect was confirmed as an important factor influencing the tool wear process during particleboard milling. This material property has not been considered in previous studies [4, 5].

**Key Words:** Melamine Coated Particle Board, Milling, Cemented Carbide, Cutting Edge Wear, High Temperature Corrosion

## INTRODUCTION

In previous work [5], the authors presented an experimental study of the influence of the average content and size of hard mineral contamination for three different particleboards manufactured industrially. The particleboards were milled with different cutting paths, sharpness and rake angles. High variation of machining properties that could not be explained only by mineral contamination was observed (Fig. 1). The cutting edge wear process is affected by a supposed presence of an unrecognized chemical wear.

Other impacts on the cutting edge wear of several particle board properties have been excluded, namely: resin and filler content in melamine film and its micro-hardness.

In the present study, the HTC effect of a particle board towards the binder in cemented carbide, expressed by quantifier ( $R_{MSMI}$ ), was added to the previous experimental matrix analyzed in [5]. A new mesh analysis of the hard mineral contamination was performed. The experimental matrix was also expanded by a relative, two-dimensional macro porous share ( $P_S$ ). A new multivariable analysis was performed, resulting in the complete model for the three examined particleboards.

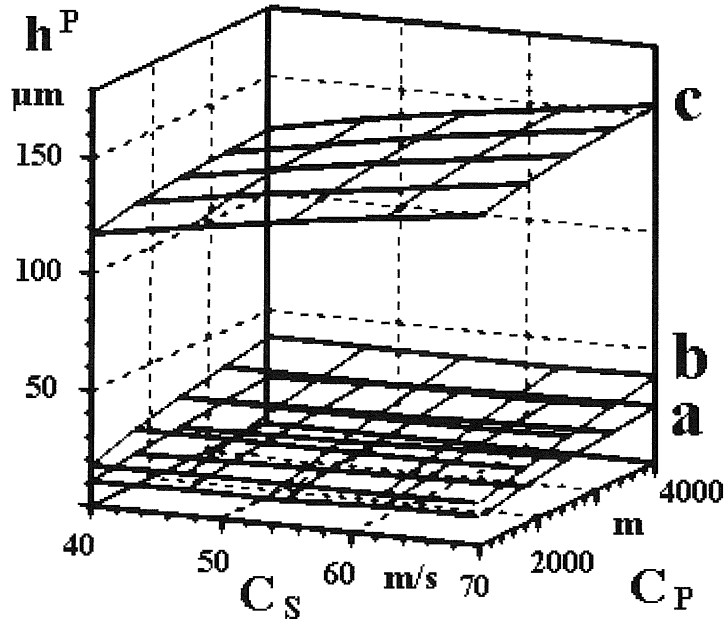


Fig. 1. The plot of the cutting edge wear ( $h^P$ ), versus the cutting path length ( $C_P$ ) and the cutting speed ( $C_S$ ), predicted from: a-model (6); b-model (7); c-model (8) for three different coated particle boards [5]

## MATERIALS AND METHODS

The melamine coated particle boards analyzed in the previous study [5] were used, as well as three new particleboards and a sample of Scots pine (*Pinus silvestris*) wood were examined, to investigate the HTC effect towards a binder of cemented carbide. To evaluate the ( $R_{MSMI}$ ) quantifier, a method presented in work [2] was used. The material of the cutting edge was the cemented carbide K05 produced by Leuco, Germany. The hard contamination particles were separated into fractions using 1500, 600, 400, 200, 100 and 50  $\mu\text{m}$  steel meshes. The two biggest fractions of contamination particles were excluded for evaluation of ( $S_{AC}$ ) and ( $W_{ASS}$ ). The ( $W_{ASS}$ ) was estimated for six fractions. In the actual study, the ( $S_{AC}$ ) for a skin was used instead of the average content of hard mineral contamination. Results of the analysis show that the ( $S_{AC}$ ) for the skin is about twice as high as average one. The relative, two-dimension macroporous share ( $P_S$ ) was evaluated by a tool microscope.

A multifactorial, non-linear regression analysis of the experimental matrix expanded by the ( $R_{MSMI}$ ) quantifier was performed. The quality of approximation was checked using: a summation of residuals square (SK), the average deviation from the regression curve (SR), and the variation (V).

For data processing, a computer optimization program, based on gradient-random method

Table 1 The correlation coefficient ( $R$ ), average deviation from regression curve ( $SR$ ), the summation of residuals square ( $SK$ ), the variance ( $V$ )

$R$	$SR \mu\text{m}$	$SK$	$V$
0.99	3.06	337	8.9

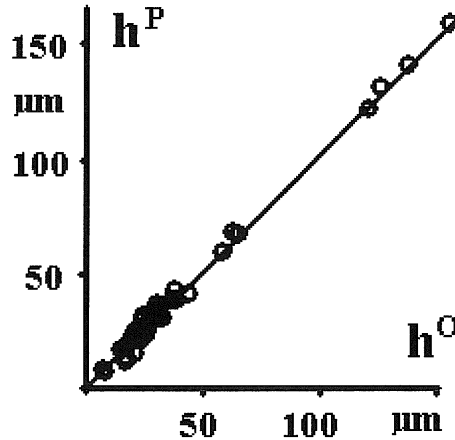


Fig. 2. The plot of the cutting edge wear ( $h^P$ ), predicted from formulas (1) versus the wear ( $h^O$ ) observed

developed in [1] with further changes [3] was used. Calculations were performed at the Poznań Supercomputing and Networking Center (PCSS) on an IBM PS-2 computer.

## RESULTS AND DISCUSSION

The model (1) is an generalization of the relation between cutting edge wear, the properties of material being machined and the cutting parameters,  $h^P = f(C_P, C_S, \beta_F, \gamma_F, S_{AC}, W_{ASS}, R_{MSMI}, P_S)$ , when milling coated particle board longitudinal:

$$\begin{aligned}
 h^P = & 8.5 \cdot 10^{-3} \cdot 0.318^{\gamma_F} \cdot \beta_F^{-1.001} \cdot C_S^{0.205} \cdot S_{AC}^{0.293} \cdot W_{ASS}^{1.3756} \cdot R_{MSMI}^{-0.0275} - 7.89 \cdot 10^{-5} \cdot C_S \cdot W_{ASS}^{1.606} \\
 & + 3.786 \cdot C_P \cdot R_{MSMI}^{2.375} + 0.174 \cdot \gamma_F \cdot W_{ASS}^{1.282} - 42.386 \cdot S_{AC}^{1.397} \cdot P_S^{5.246} \\
 & - 4.759 \cdot R_{MSMI} \cdot W_{ASS}^{1.220} [\mu\text{m}]; h^P > 0
 \end{aligned} \quad (1)$$

The cutting edge wear increases with increase in the content ( $S_{AC}$ ) and particle size of the hard mineral contamination ( $W_{ASS}$ ) over whole range of variation (Fig. 5). The influence on edge wear of the corrosivity of the machined material towards tool material is represented by the quantifier ( $R_{MSMI}$ ). This increases with increase in the cutting path length ( $C_P$ ) (Fig. 4). Following the ( $C_P$ ) increase, the impact of  $R_{MSMI}$  on cutting edge wear increases with temperature

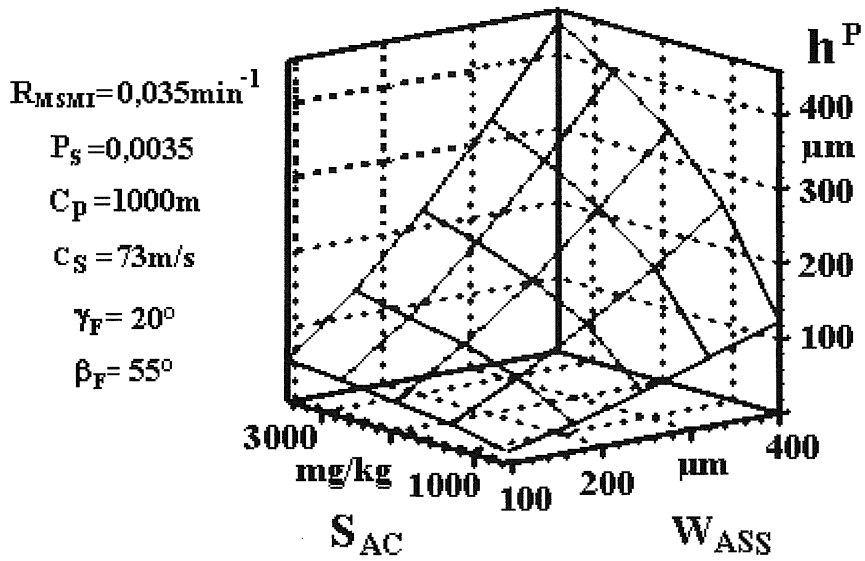


Fig. 3. The plot of the cutting edge wear ( $h^P$ ), predicted from the model (1), versus the content of hard mineral contamination ( $S_{AC}$ ) and the weighted average size of contamination particles ( $W_{ASS}$ )

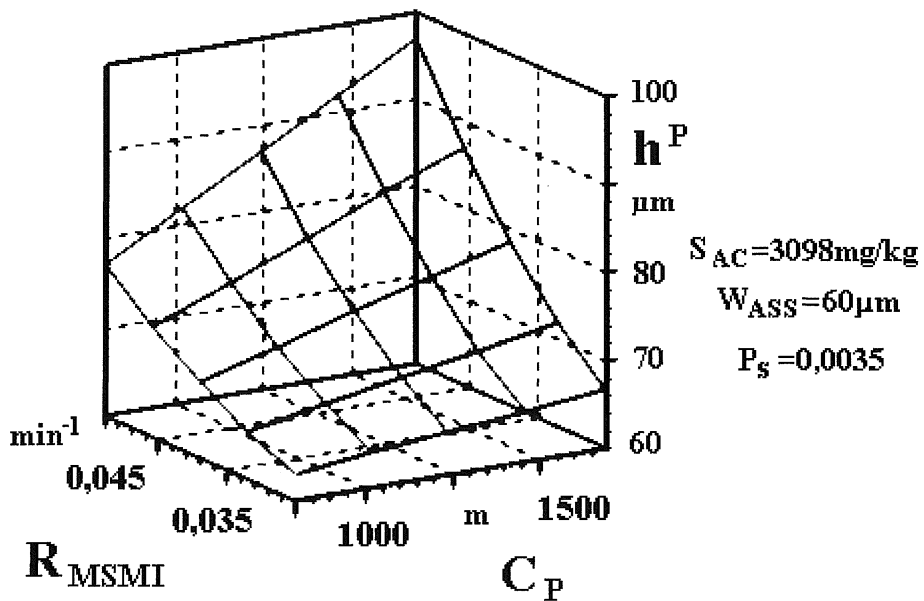


Fig. 4. The plot of the cutting edge wear ( $h^P$ ), predicted from model (1), versus the corrosivity of particle board ( $R_{MSMI}$ ) and the cutting path length ( $C_P$ )

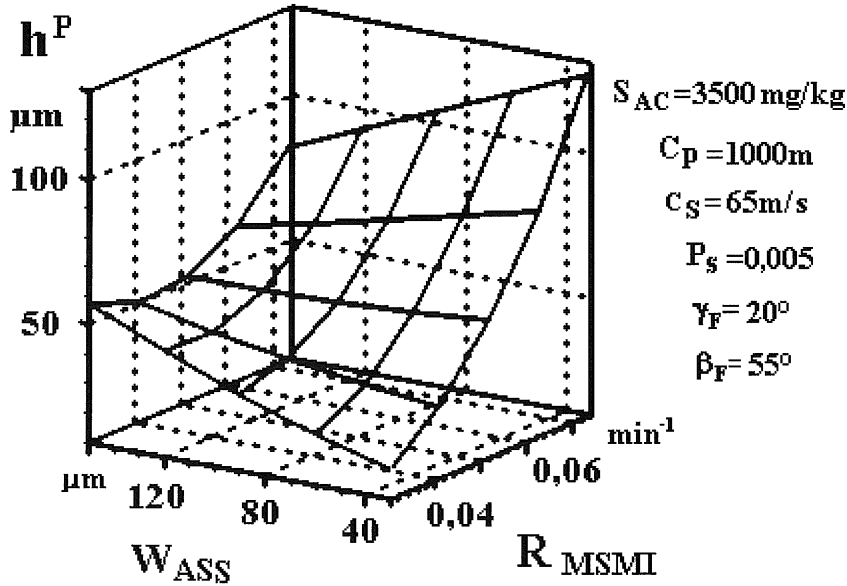


Fig. 5. The plot of cutting edge wear ( $h^P$ ), predicted from model (1), versus the weighted average size of hard contamination particles ( $W_{ASS}$ ) and the corrosivity of particle boards ( $R_{MSMT}$ )

in the cutting zone. The role of ( $R_{MSMT}$ ) decreases with increase of ( $W_{AS}$ ) (Fig. 5). The reason for this behaviour is probably creation of notches (loss of many WC grains at the same time) caused by hard mineral contamination particles, bigger than the WC grain size, and indentation into the surface machined during the cut. At the bottom of the notches, until their smoothing, the pressure on the cutting edge diminishes, resulting in reduction of the HTC. The increase of porous share ( $P_S$ ) decreases the cutting edge wear with an interaction term  $S_{AC} \cdot P_S$ . The porosity causes less strengthening of particles of hard mineral contamination in the structure of a particleboard.

Over the whole range of variation, the cutting edge wear ( $h^P$ ) increases with decrease of the sharpness angle ( $\beta_F$ ) (Fig. 6). Below  $\beta_F = 45^\circ$  this effect is much more rapid, and speeds up with reduction of rake angle ( $\gamma_F$ ). The influence of the rake angle ( $\gamma_F$ ) on the cutting edge wear ( $h^P$ ) (Fig. 6) is complex. A minimum cutting edge wear ( $h^P$ ) can be observed for certain values of the ( $\gamma_F$ ). However, the minimum increases with increase in ( $Z_{ZM}$ ) and ( $S_{WRZ}$ ). For the lowest ( $Z_{ZM}$ ) and ( $S_{WRZ}$ ), the minimum of ( $h^P$ ) was observed for  $\beta_F = 9^\circ$ . According to this finding, it can be stated that the optimal rake angle for coated particle board milling presented in the literature [6], where content and size of the mineral contamination was not varied, has no general applicability.

Increase in the cutting path ( $L_S$ ) causes a proportional increase of the cutting edge wear ( $h^P$ ) (Fig. 7). This is different from previous observations [4,5]. An explanation of the HTC properties of material machined, expressed by quantifier ( $R_{MSMT}$ ), is included in the model (1).

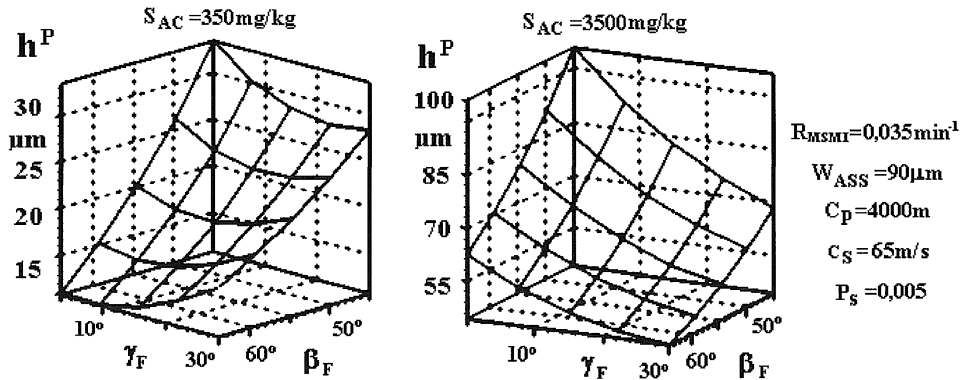


Fig. 6. The plot of the cutting edge wear ( $h^P$ ), predicted from the model (1), versus the rake ( $\gamma_F$ ) and the sharpness angles ( $\beta_F$ )

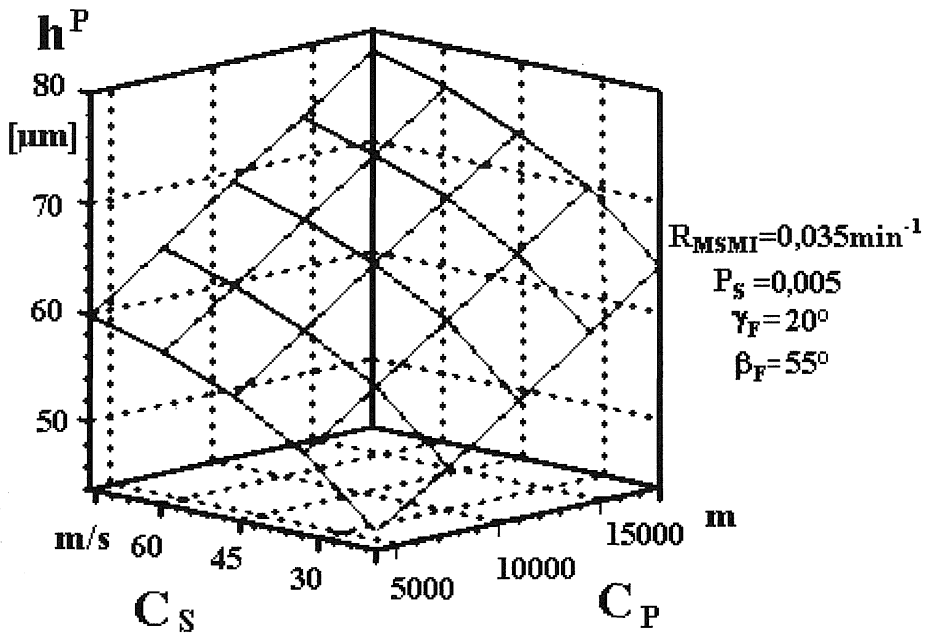


Fig. 7. The plot of cutting edge wear ( $h^P$ ), predicted from model (1), versus cutting speed ( $C_S$ ) and cutting path length ( $C_P$ )

The increase of the cutting speed ( $C_S$ ) results in increase in the cutting edge wear ( $h^P$ ) (Fig. 7). This applies to the whole range of variation of ( $C_S$ ), and is in agreement with previous works [3,5,6]. An interaction term of ( $W_{ASS}$ ) with the ( $C_S$ ) on the ( $h^P$ ) was derived. The role of the

cutting speed is not large compared to the role of other variables.

## CONCLUSIONS

1. The quantifier describing the HTC properties of coated particle boards ( $R_{MSMI}$ ) was used to develop a generalized model of the relationship between cutting edge wear ( $h^P$ ), stereometrical parameters of the cutting edge, machining parameters as well as some properties of material machined in case of different particle boards.

2. The size of particles ( $W_{ASS}$ ) and the content ( $S_{AC}$ ) of hard mineral contamination are important factors influencing the cutting edge wear ( $h^P$ ).

3. The cutting edge wear ( $h^P$ ) highly depends on the sharpness angle ( $\beta_F$ ), especially below  $\beta_F=45^\circ$ . The cutting edge wear ( $h^P$ ) decreases with increase of ( $\beta_F$ ) over the whole examined range.

4. The influence of the rake angle ( $\gamma_F$ ) on cutting edge wear ( $h^P$ ) is complex. The minimum ( $h^P$ ) for certain values of ( $\gamma_F$ ), increasing with increasing ( $Z_{ZM}$ ) and ( $S_{WRZ}$ ), can be observed. For the lowest ( $Z_{ZM}$ ) and ( $S_{WRZ}$ ) the minimum value of ( $h^P$ ) was observed by  $\beta_F=9^\circ$ .

5. The cutting edge wear ( $h^P$ ), while milling coated particle boards, depends not only from variables examined ( $C_P, C_S, \beta_F, \gamma_F, R_{MSMI}, S_{AC}, W_{ASS}, P_S$ ), but also from several interaction terms:  $C_P \cdot R_{MSMI}$ ;  $\gamma_F \cdot W_{ASS}$ ;  $C_S \cdot W_{ASS}$ ;  $S_{AC} \cdot P_S$ ;  $R_{MSMI} \cdot W_{ASS}$ , making problem analyzed very complex.

6. The cutting path ( $C_P$ ) proportionally impacts the cutting edge wear ( $h^P$ ).

7. Over the whole range of variation, increase in cutting speed ( $C_S$ ) increases the cutting edge wear ( $h^P$ ).

8. Increase in porous share ( $P_S$ ) decreases the cutting edge wear ( $h^P$ ).

## ACKNOWLEDGEMENTS

The authors acknowledge following grants: at the Poznań Supercomputing and Networking Center (PCSS), Poznań, Poland, and at American-Polish Maria Skłodowska-Curie II Fund in Warsaw, Poland.

## LITERATURE CITED

1. Porankiewicz B. (1988): Mathematical Model of Edge Dullness for Prediction of Wear of Wood Cutting Tools. Proc. 9<sup>th</sup> IWMS, UC, Berkeley CA, USA: 169–170.
2. Porankiewicz B. (1997): The Simulation of High Temperature Corrosion of Components of Cemented Carbide Cutting Edge in Contact with Particle Board. Proc. of 13<sup>th</sup> IWMS, Vancouver, Canada: 779–790.
3. Porankiewicz B. (2000): Zużycie ostrzy narzędzi przy frezowaniu płyt wiórowych. Wydawnictwo Poznańskiego Towarzystwa Przyjaciół Nauk, Poznań, Poland, pp: 113.
4. Porankiewicz B., Grönlund A. (1991): Tool Wear-Influencing Factors. Proc. of 10<sup>th</sup> IWMS, UC Berkeley, CA, USA: 220–229.

5. Porankiewicz B., Tanaka C. (1993): The Workability of Melamine Coated Particle Board. Faculty of Agriculture, Shimane University, Matsue, Japan, 27: 57-63.
6. Stühmeier W (1989) Fräsen von Spanplatten mit hochharten Schneidstoffen. no. 181, pp. 191. TU Braunschweig: F-B VDI R.2